We are IntechOpen, the world's leading publisher of Open Access books
Built by scientists, for scientists

4,800
Open access books available

122,000
International authors and editors

135M
Downloads

Our authors are among the

154
Countries delivered to

TOP 1%
most cited scientists

12.2%
Contributors from top 500 universities

CLARIVATE ANALYTICS
BOOK CITATION INDEX
INDEXED

WEB OF SCIENCE™

Selection of our books indexed in the Book Citation Index
in Web of Science™ Core Collection (BKCI)

Interested in publishing with us?
Contact book.department@intechopen.com

Numbers displayed above are based on latest data collected.
For more information visit www.intechopen.com

Techniques for Tuning BAW-SMR Resonators for the 4ᵗʰ Generation of Mobile Communications

M. El Hassan, E. Kerherve, Y. Deval, K. Baraka, J.B. David and D. Belot

Additional information is available at the end of the chapter

1. Introduction

In telecommunication systems, all filters and resonators that constitute the RF part have the tendency to be integrated on the same chip that contains the information treatment.

In order to achieve miniaturization, bulk acoustic wave (BAW) technology is presented. BAW filters are very sensitive to surface contamination, and can exhibit very small sizes. In addition, BAW resonators could be fabricated using compatible material CMOS and BiCMOS [1]. In this context and in order to compensate the variation due to the fabrication process, the work presented in this paper focuses on the tuning of BAW-SMR resonators and filters.

This work is divided in two parts. The first part consists of designing BAW-SMR (Solidly Mounted Resonator) filters. In the second part, we propose the use of two methods to tune this type of filters. Thus, we present the design methodology, the study, and the experimental realization of the BAW-SMR tunable filters.

2. BAW impedance behavior

2.1. SMR impedance behavior

The bulk acoustic wave resonator is basically constituted by a piezoelectric layer sandwiched between two electrodes (Fig.1). The application of an electric field between the two electrodes generates a mechanical stress that is further propagated through the bulk of the structure (acoustic wave). The resonance condition is established when the acoustical path (in thickness direction) corresponds to odd integer multiples of the half acoustic wavelength. The bulk acoustic wave resonator is basically constituted by a piezoelectric layer sandwiched between two electrodes (Fig.1) [2, 3].

The bulk acoustic wave resonator fabrication over silicon substrates imposes its acoustical isolation, confining the acoustic waves into the main resonant structure. Two configurations are proposed: the membrane suspended structure (FBAR – Film Bulk Acoustic wave Resonator) [3], where the resonator is suspended by an air-bridge (Fig.1a); and the solidly-mounted structure (SMR – Solidly Mounted Resonator), where the resonator is mounted over a stack of alternating materials (Fig.1b). This stack is built on a Bragg reflector basis and it has an acoustic mirror behavior [2-3]. Both, air and acoustic mirror, present an optimum discontinuity for reflecting the acoustic waves at the interface with the bottom electrode, confining waves into the main resonant structure.

In the solidly mounted resonator (SMR), the piezoelectric is solidly mounted to the substrate (Fig.1.b). Some means must be used to acoustically isolate the piezoelectric from the substrate if a high quality factor (Q) resonance is to be obtained. In effect, the quarter wavelength layers act as a reflector to keep waves confined near the piezoelectric transducer film [4]. The effect of the reflector on mechanical displacement is to cause the wave amplitude to diminish with depth into the reflector. The number of layers required to obtain a satisfactory reflection coefficient is dependent on the mechanical impedances between layers and, to a lesser extent, the substrate [5]. The number of layers is best determined by an analysis of the resonance response as a function of the number of layers versus resonator 'Q' and coupling coefficient.
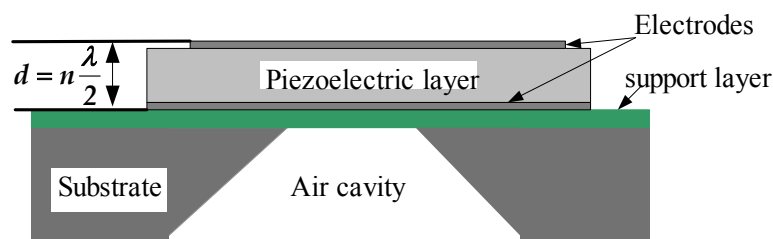

(a)
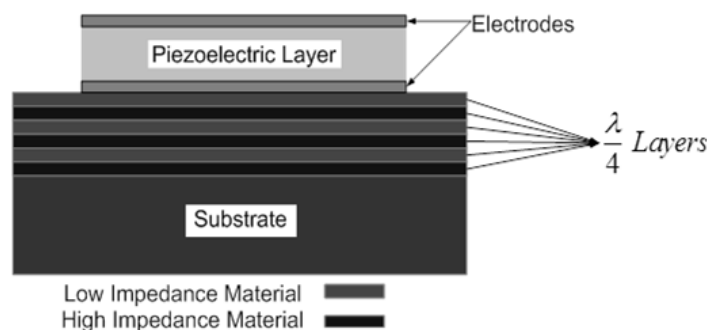
(b)

Figure 1. (a) Film Bulk Acoustic Resonator (FBAR). (b) Solidly Mounted Resonator (SMR).

An important effect of the reflector layers, as demonstrated by Newell [4], is a partial lateral stiffening of the piezoelectric plate that minimizes plate wave generation and spurious resonances normally observed in free plates. However, real resonator structures are inherently 3D and some form of radiation beyond the simple thickness dimension is to be expected. If energy leaves the resonator structure, through radiation, then it counts as a loss mechanism. Reflections of lateral waves at the edge of the resonator can lead to standing waves and spurious responses. The SMR approach requires that the substrate be smooth in order to proceed with the fabrication of reflectors, electrodes, and piezoelectric film [5].

2.2. The Butterworth-Van-Dyke (BVD) model

The Modified Butterworth-Van-Dyke (MBVD) model is an electrical schematic around resonance (Fig.2). The elements R_a, L_a, C_a present the series resonance and the insertion losses. The capacity C_0 represents the piezoelectric material between the two electrodes.
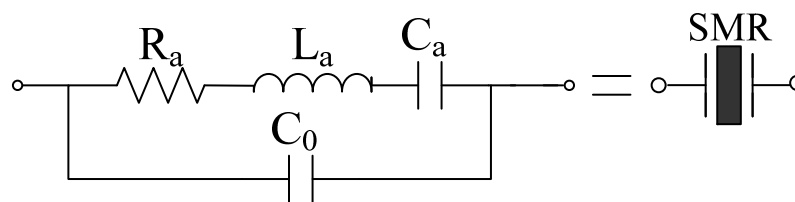
Figure 2. SMR-MBVD model.

The impedance characteristic of a measured BAW-SMR is shown in Fig.3. In this graph, it can be observed that the SMR presents mainly two resonance pulsations: the series resonance (f_s), when the electrical impedance approaches to zero, and the parallel resonance (f_p), when the electrical impedance approaches to infinity. For all other frequencies far from
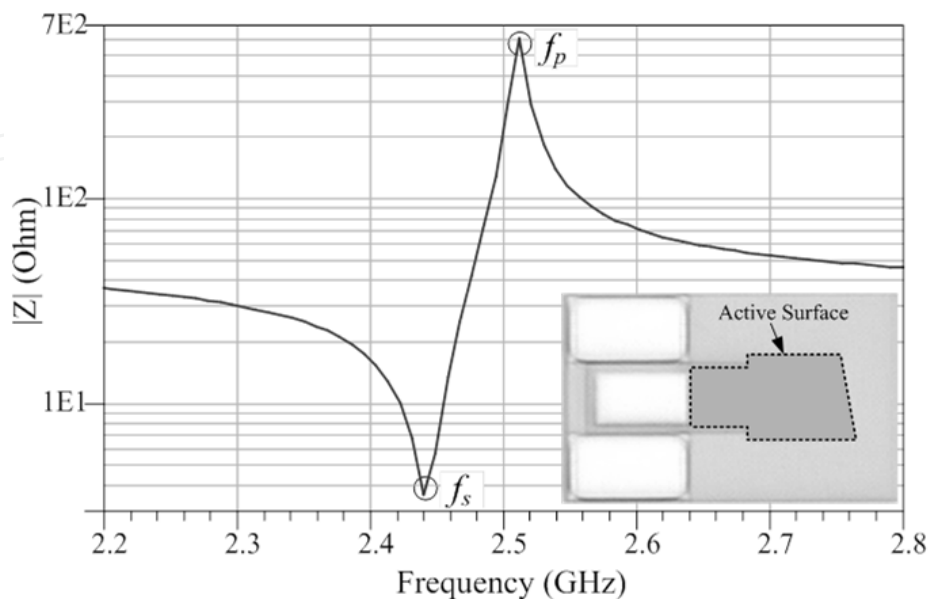
Figure 3. Impedance characteristic of a measured BAW-SMR.

the resonances, the SMR presents static capacitor behavior. f_s is adjusted according to the thickness of the piezoelectric layer and it is spaced by the parallel resonance f_p. The instantaneous frequency deviation between the two resonances is determined by the electromechanical coupling coefficient of the piezoelectric layer. The quality factor of the measured BAW-SMR is 192.5 and its active area is 16800 μm^2. This relatively small quality factor is due to some technological problems.

The electrical impedance of an SMR is obtained by solving the acoustic boundary problem and applying the transmission line theory [6]. The electrical SMR impedance can be simplified and expressed by the following equation:

$$Z_{SMR} = \frac{1}{sC_0} \frac{(f^2 - f_s^2)}{(f^2 - f_p^2)} \tag{1}$$

where 's' is the complex variable: s = jw.

2.3. Addition of external passive elements

The association of external passive components (L, C) to the resonators was made in two parts. First, the resonators analyses have been carried out using on-wafer measurements. Then, these results have been associated with the capacitors and inductors. The combination of experimental results and modeling of passive elements constitutes the final response of the tuned resonators.

2.3.1. Addition of capacitors

The addition of the capacitors (having an intrinsic quality factor 'Q' > 140) to the SMR circuitry doesn't affect severely the quality factor of the overall design. The resonator's electromechanical coupling coefficient is described indirectly by the capacitor ratio C_0/C_a as determined by the resonator physical configuration and piezoelectric material properties [7]. When changing the electromechanical coefficient of the piezoelectric material, the bandwidth changes. Our goal is to tune the capacitor ratio C_0/C_a by adding series or parallel capacitors to the resonator. Thus, controlling this ratio will enable us to control the electromechanical coefficient, and as a sequence the bandwidth of the resonator.

2.3.1.1. Series capacitor association

The performance analysis of the association of series capacitor to the SMR is based on the BVD model (Fig.4). The analysis of the frequency response of the series capacitor associated to the SMR will lead us to (2) presented below:
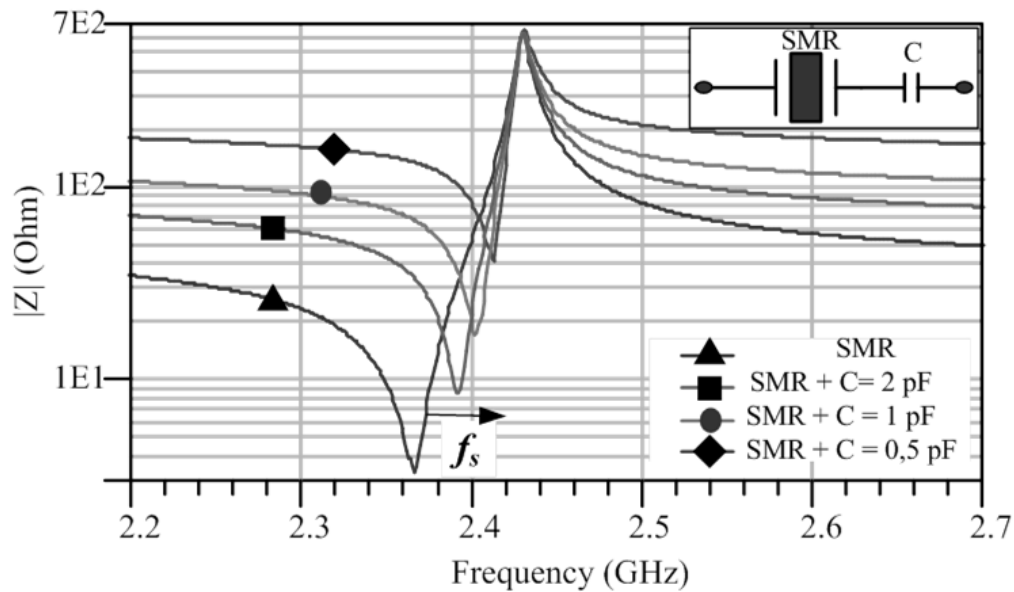
$$Z_{in} = \frac{s^2(CC_aL_a + C_0C_aL_a) + C_0 + C_a + C}{sC(s^2C_0C_aL_a + C_0 + C_a)} \tag{2}$$

Where 's' is the complex variable: s = jw.

From (2), it is possible to notice the insertion of a pole and zero to the frequency response of the simple resonator. The extraction of the poles and zeroes values of (2), will lead us to (3) & (4) shown below.

$$f_s = \frac{1}{2\pi}\sqrt{\frac{C_0 + C_a + C}{CC_a L_a + C_0 C_a L_a}} \tag{3}$$

$$f_p = \frac{1}{2\pi}\sqrt{\frac{C_0 + C_a}{C_0 C_a L_a}} \tag{4}$$

Figure 4. Impedance response of the measured BAW-SMR with series capacitor.
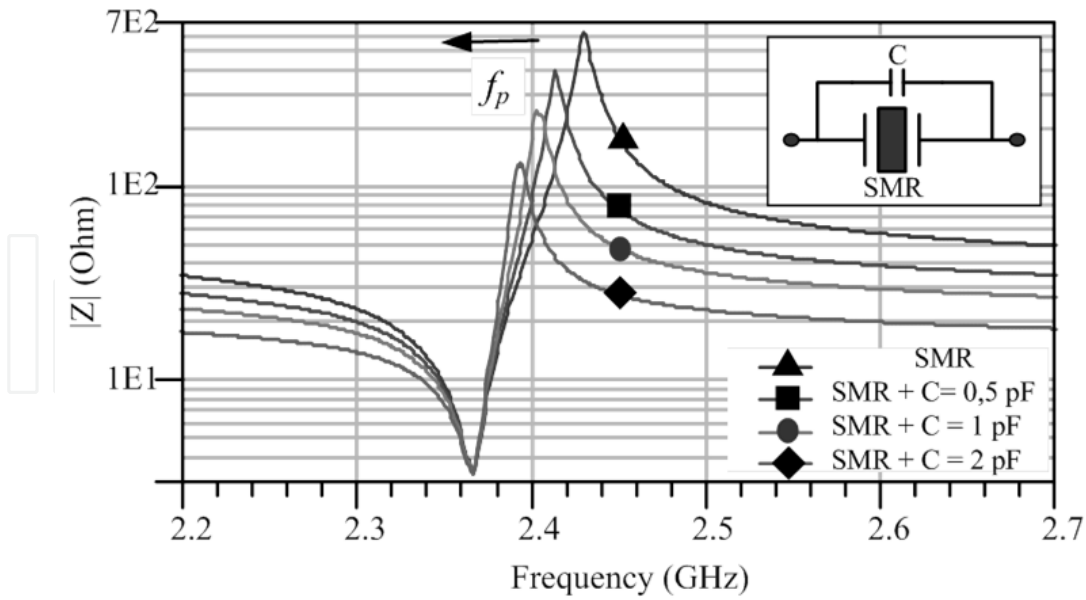
From (3) & (4), it may be noted that the capacitor added in series with the BAW resonator affects only the series resonance frequency. It is inversely proportional to f_s. To illustrate this theoretical study, responses with different values of capacitors added in series with the measured BAW-SMR are shown in Fig.4.

2.3.1.2. Parallel capacitor association

The analysis of the frequency response of the parallel capacitor associated to the SMR will lead us to (5), presented below.

$$Y_{in} = \frac{s(s^2 L_a C_a(C_0 + C) + C_0 + C + C_a)}{s^2 L_a C_a + 1} \tag{5}$$

$$f_s = \frac{1}{2\pi}\sqrt{\frac{1}{C_a L_a}} \tag{6}$$

Figure 5. Impedance response of the measured BAW-SMR with parallel capacitors.

$$f_p = \frac{1}{2\pi}\sqrt{\frac{C_0 + C_a + C}{L_a C_a (C_0 + C)}} \qquad (7)$$

From (5), it is possible to notice the displacement of the poles of the device's resonance frequency. The extraction of the poles and zeroes values of (5), will guide us to (6) & (7) as shown below.

It is noticed from (6) & (7) that the capacitor added in parallel with the BAW resonator affects only the parallel resonance frequency. It is inversely proportional to f_p. Fig.5 presents the final responses of the measured BAW-SMR with different values of capacitors added in parallel.

2.3.2. Addition of inductors

The association of inductors to the BAW resonators could be realized in series or parallel. We should note that in the case of VLSI-CMOS, these inductors are characterized by a small quality factor with respect to the BAW (400 to 1000) which degrades the quality factor of the overall circuitry, and they occupy a relatively large size.

2.3.2.1. Series inductor association

The performance analysis of the assembly of the inductors in series with the SMRs is based on the BVD model. The analysis of the frequency response of the series inductors associated to the SMR will lead us to (8).

$$Z_{in} = \frac{s^4 C_0 C_a L_a L + s^2 (C_a L_a + C_0 L + C_a L) + 1}{s(s^2 C_a L_a C_0 + C_0 + C_a)} \qquad (8)$$

From (8), it is possible to notice the insertion of a zero to the resonator frequency response. The extraction of the poles and zeroes values from (8), will bring (9) & (10). Based on these equations, we can see that the values of the poles are not deteriorated. However, from (9), we notice that the association of series inductors to the SMR will modify the zeroes, and only the series resonance frequency is affected. It is inversely proportional to f_s.
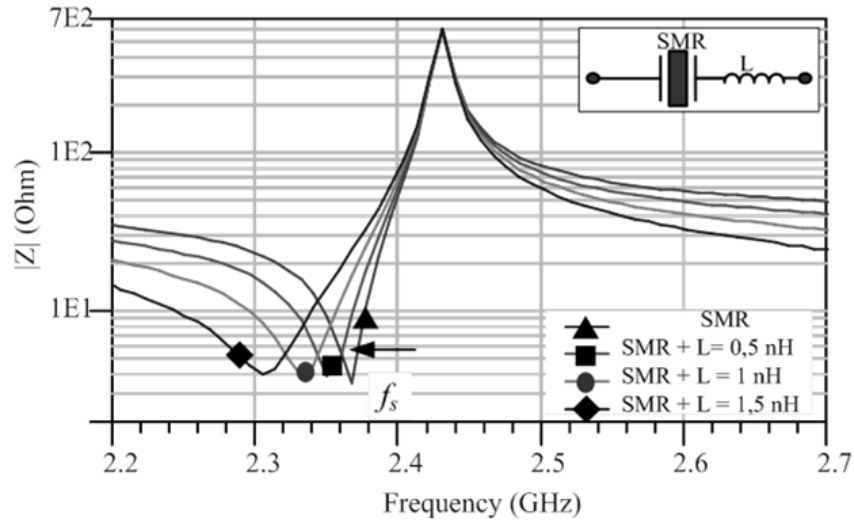
Figure 6. Impedance response of the measured BAW-SMR with series inductors.

To illustrate this theoretical study, impedance behavior of the measured BAW-SMR with different values of inductors associated in series is shown in Fig.6.

$$f_s = \frac{1}{2\pi} \sqrt{\frac{(C_a L_a + C_0 L + C_a L) \pm \sqrt{(C_a L_a + C_0 L + C_a L)^2 - 4C_0 C_a L_a L}}{2C_0 C_a L_a L}} \tag{9}$$

$$f_p = \frac{1}{2\pi} \sqrt{\frac{C_0 + C_a}{C_a L_a C_0}} \tag{10}$$

*2.3.2.2. Parallel inductor association*

Based on the same procedure used above, the analysis of the frequency response of the parallel inductors associated to the SMR will lead us to (11), presented below.

$$Y_{in} = \frac{s^4 C_0 C_a L_a L + s^2 (C_0 L + C_a L + C_a L_a) + 1}{sL(1 + s^2 C_a L_a)} \tag{11}$$

From (11), it is possible to notice the insertion of a pole to the resonator frequency response and the displacement of another. Also, we can notice the composition of a double pole near the frequency response of the device. The extraction of the poles and zeroes values from (11), will lead us to (12) & (13).

From (12) & (13), we can see that that the inductor added in parallel with the BAW resonator affects only the parallel resonance frequency. It is inversely proportional to f_p. Fig.7 presents the final responses of the measured BAW-SMR with different values of inductors associated in parallel.
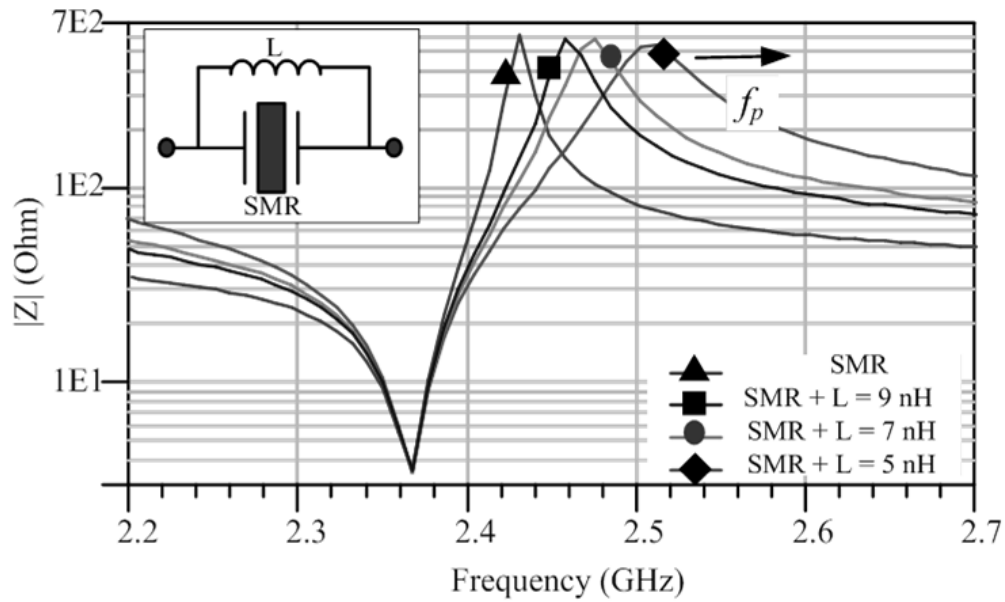
Figure 7. Impedance response of the measured BAW-SMR with parallel inductors.

$$f_p = \frac{1}{2\pi}\sqrt{\frac{\left(C_0 L + C_a L + C_a L_a\right) \pm \sqrt{\left(C_0 L + C_a L + C_a L_a\right)^2 - 4C_0 C_a L_a L}}{2C_0 C_a L_a L}} \qquad (12)$$

$$f_s = \frac{1}{2\pi}\sqrt{\frac{1}{C_a L_a}} \qquad (13)$$
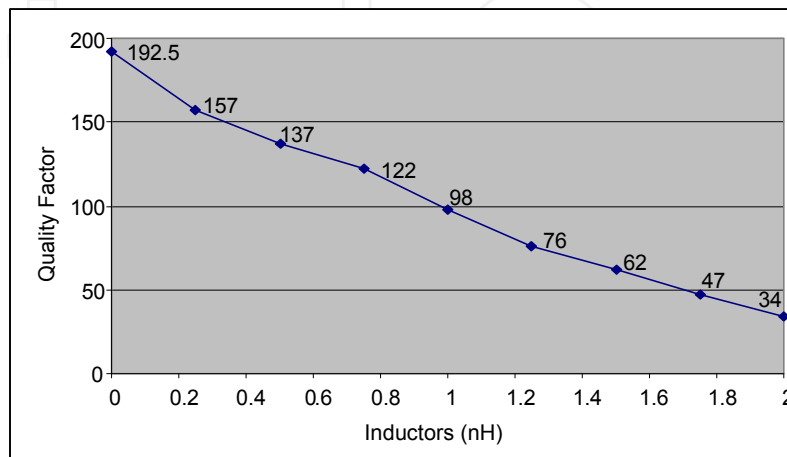
Figure 8. Impact of the quality factor of the inductors added in series with the BAW resonator on the series quality factor 'Q_s' of the overall resonator circuitry (SMR+L).

The addition of inductors to the BAW-SMR increases the insertion losses and degrades the quality factor of the overall circuitry. Fig.8 illustrates the influence of inductors added in series with the SMR on the overall quality factor of the assembly.

3. BAW filter design

3.1. Bulk Acoustic Wave (BAW) filters topologies

Bulk acoustic wave filters are basically divided in three topologies: ladder, lattice and ladder-lattice (Fig.9) [3].
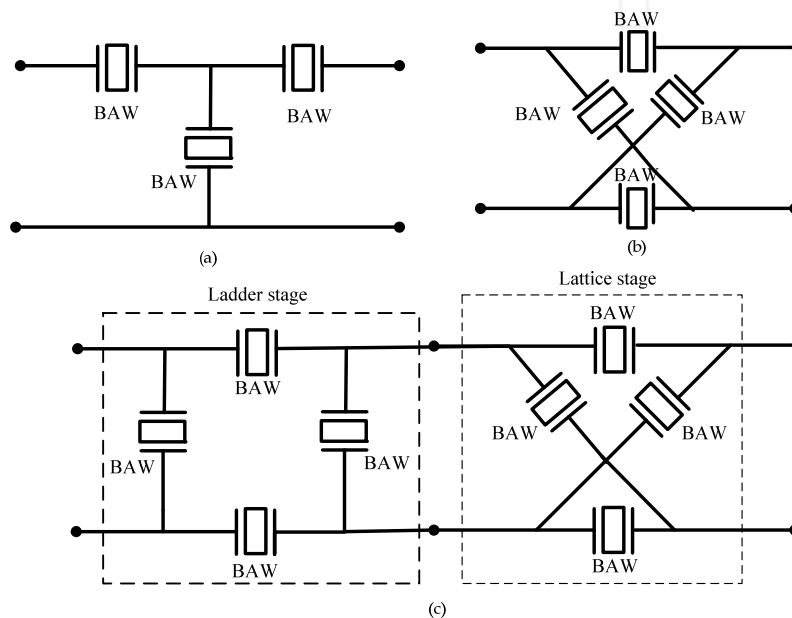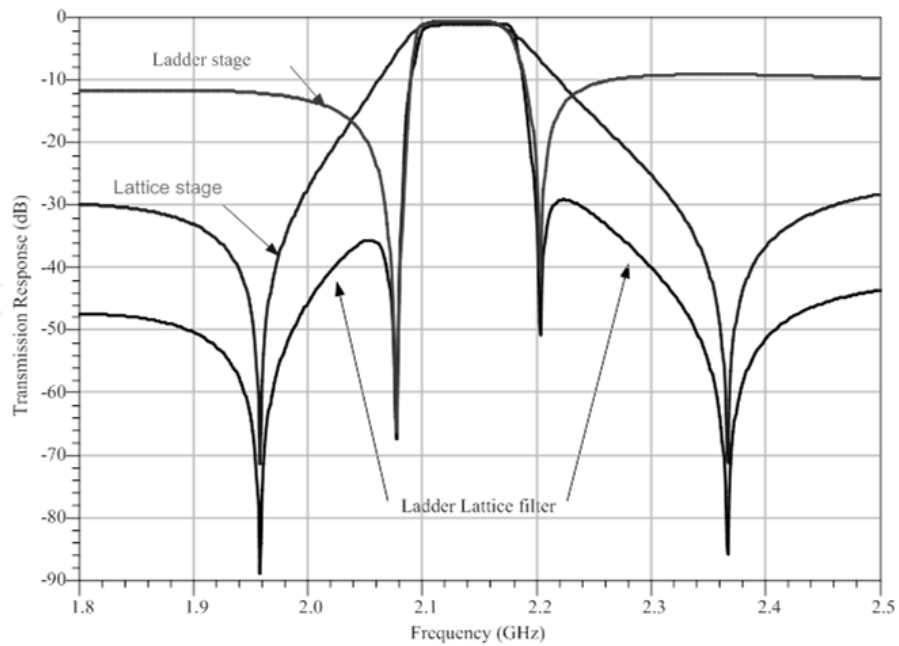

Figure 9. Bulk acoustic wave resonator filter topologies: (a) ladder stage, (b) lattice stage and (c) ladder-lattice stage.

Ladder filter are characterized by an unbalanced operation mode and very small size able to deliver very high selectivity filtering responses, however presenting low rejection or isolation out-of-band. Typically, ladder bulk acoustic wave filters are quite effective for blocking signals close to the passband, but poor at rejecting undesired bands [3-4].

On the other hand, lattice bulk acoustic wave filters are characterized by a balanced operation mode. In contrast to the first one, this topology presents typically a low selectivity close to the passband, followed by a high rejection out-of-band. They present slower roll off coefficient and higher rejection. Thus, lattice networks are not interesting to block signals close to the passband, but they are more effective for rejecting undesired bands [3].

Ladder-lattice bulk acoustic wave filters are also characterized by a balanced operation mode. Ladder-lattice filters ally advantages of both network types, enabling high isolation at undesired bands and steep responses close to the passband [3]. This topology is able to strongly reduce the linearity constraints of the receiver RF chain. Fig.10 shows a comparison between the typical theoretical transmission responses (S_{21}) of these three network types.

Figure 10. Theoretical transmission responses for main bulk acoustic wave (BAW) filter topologies.
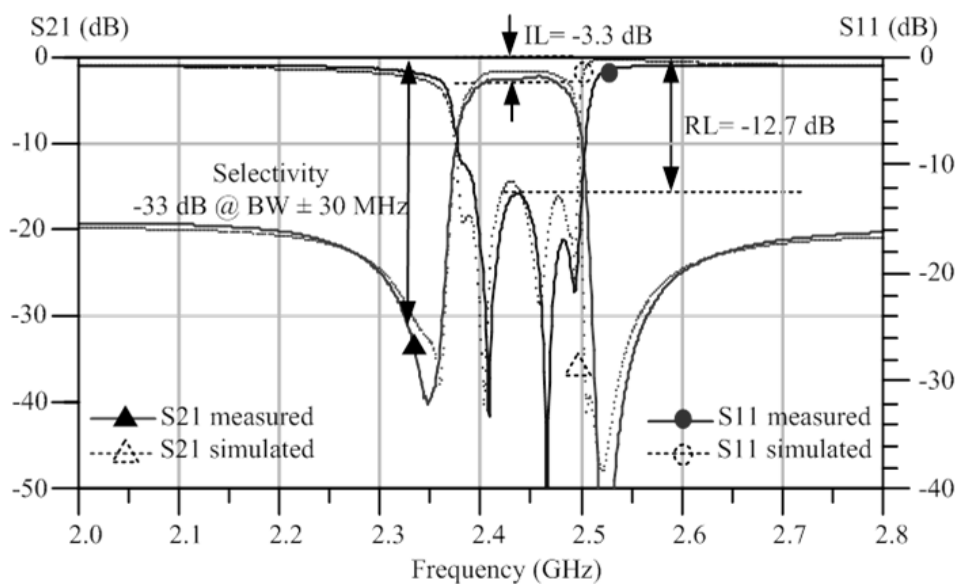
3.2. Ladder BAW-SMR filter design

The ladder filter is an association of resonators in series and in parallel. The shunt resonators are loaded and their resonance frequencies are smaller than the series resonators. Ladder BAW topology presents a good selectivity which enables to block undesired signals near the pass band. In this context, and in order to support the theoretical study, a tunable BAW-SMR ladder filter was designed for the 802.11b/g standard (2.40 – 2.48 GHz). The resonators and filters were fabricated at the CEA-Leti in the framework of the project '*EPADIM*'. The filter is composed of five SMRs, associated in ladder topology. The filter stack can be divided into resonators' layers and Bragg reflector's layers. The resonator's layers are composed by the classical couple AlN-Mo [8]. However, in contrast to [8], the Bragg reflector was implemented using an exclusive dielectric stack composed by SiOC:H and Si_xN_y [9].
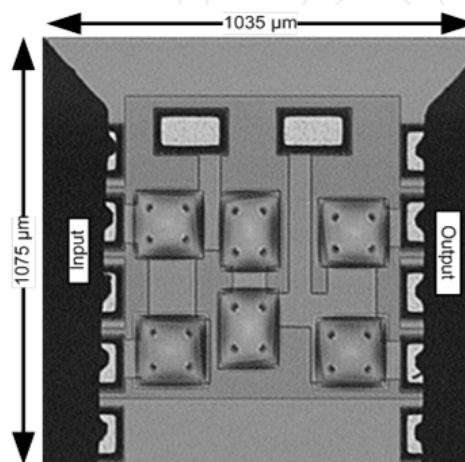
Figure 11. Microphotography of the Ladder BAW-SMR for the 802.11b/g standard.

The acoustical performance of the fully dielectric stack is comparable to the traditional SiO2-W reflectors; however, it strongly reduces the coupling between resonators through the Bragg reflector. Furthermore, the filter stack was realized on a high resistive silicon substrate in order to reduce losses due to the capacitive coupling [10].

In order to optimize the filter performance, a double resonator and apodized geometries have been used. Indeed, double resonators present large electrodes' areas, which results in lower resistive losses. Also, the filter resonators present apodized geometries in order to avoid spurious resonances caused by the parasitic lateral acoustic modes [11]. Fig.11 and 12 show the microphotography and a comparison between the measured and simulated results of the tunable ladder BAW-SMR filter, respectively. The filter occupies a small area and has reduced dimensions (1035*1075 μm^2). Electromagnetic simulation of the overall filter structure has been performed using the ADS-Momentum software. Next, the acoustical effects have been considered using the Mason Model [12] and included in the simulations.


Figure 12. Comparison between measured and simulated results of the 802.11b/g ladder BAW-SMR filter.

The filter design was realized for implementation in SiP context. The performances of the tunable BAW-SMR filter are in concordance with the simulation results. Mainly, the filter fulfills the requirements for the WLAN 802.11 b/g standard, presenting -3.3 dB of insertion loss, -12.7 dB of return loss and a selectivity higher than 33 dB at ± 30 MHz of the bandwidth. The filter high insertion losses are mainly due to the low resonators quality factor obtained in the fabrication (Q = 200). Therefore, these losses can be strongly reduced using mechanical energy concentration techniques in the resonator acoustical cavity [13].

4. Tunability of the ladder filter

The shunt resonators of the ladder filter determine the position of the zeroes at the left of the center frequency and the series resonators determine the position of the zeroes at the right of

the center frequency. Thus, changing the impedance of the parallel and series resonators leads to a change in the zeroes' positions.
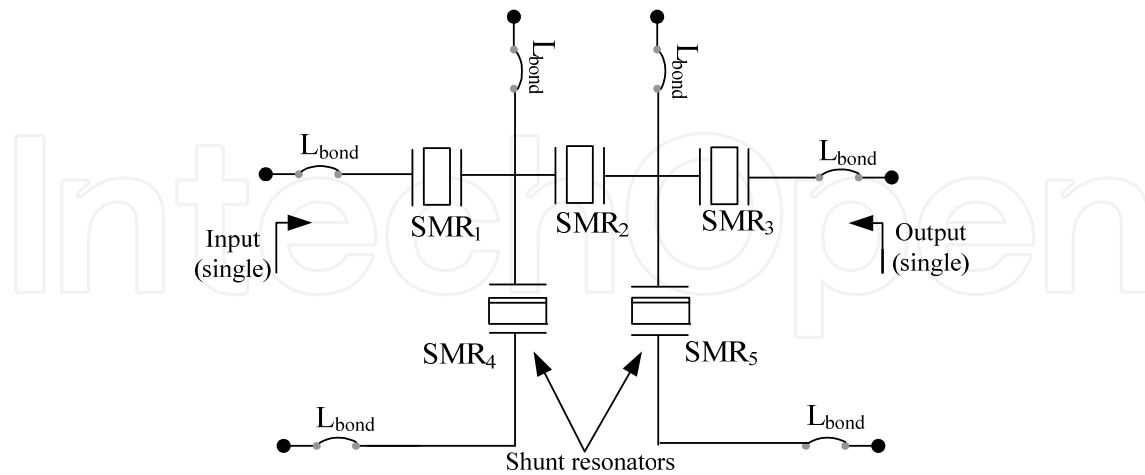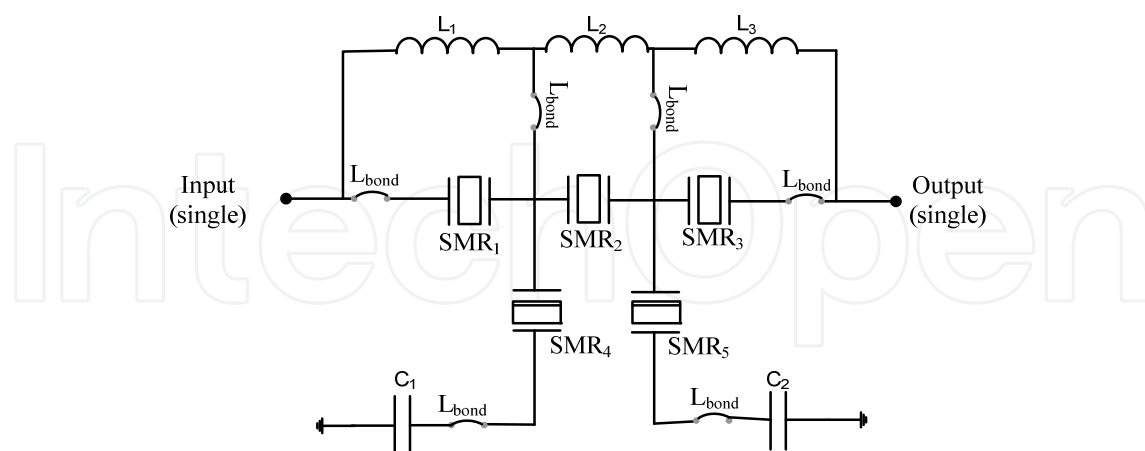

Figure 13. Ladder BAW-SMR filter.

Based on this theory and in order to tune the BAW-SMR filter (Fig.13), we propose to add passive elements to the shunt and series resonators that constitute the filter.

4.1. Shift towards higher frequencies

To shift the center frequency of the filter towards higher frequencies we have to move all the zeroes towards these frequencies. Thus, we have added inductors in parallel with the series resonators and capacitors in series with the shunt resonators that constitute the ladder BAW-SMR filter (Fig.14).
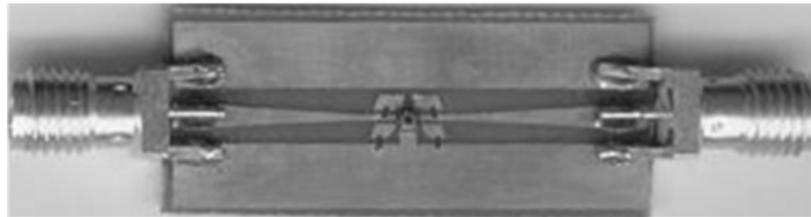

Figure 14. Tunable BAW-SMR filter with inductors added in parallel with the series resonators and capacitors added in series with the shunt resonators.

Table 1 presents the values and the quality factor of the external passive elements used in the circuitry designed to move the center frequency of the tunable BAW-SMR filter towards higher frequencies.

|	Value	Quality Factor 'Q'
Capacitors	$C_1 = C_2 = 2.2$ pF	140
Inductors	$L_1 = 3.9$ nH	47.7
	$L_2 = 5.6$ nH	40
	$L_3 = 4.7$ nH	45

Table 1. Values of the passive elements used to shift the center frequency of the tunable BAW-SMR filter towards higher frequencies and their quality factors.

The tunable BAW-SMR filter and the passive components are mounted on a FR4 substrate as shown in Fig.15.
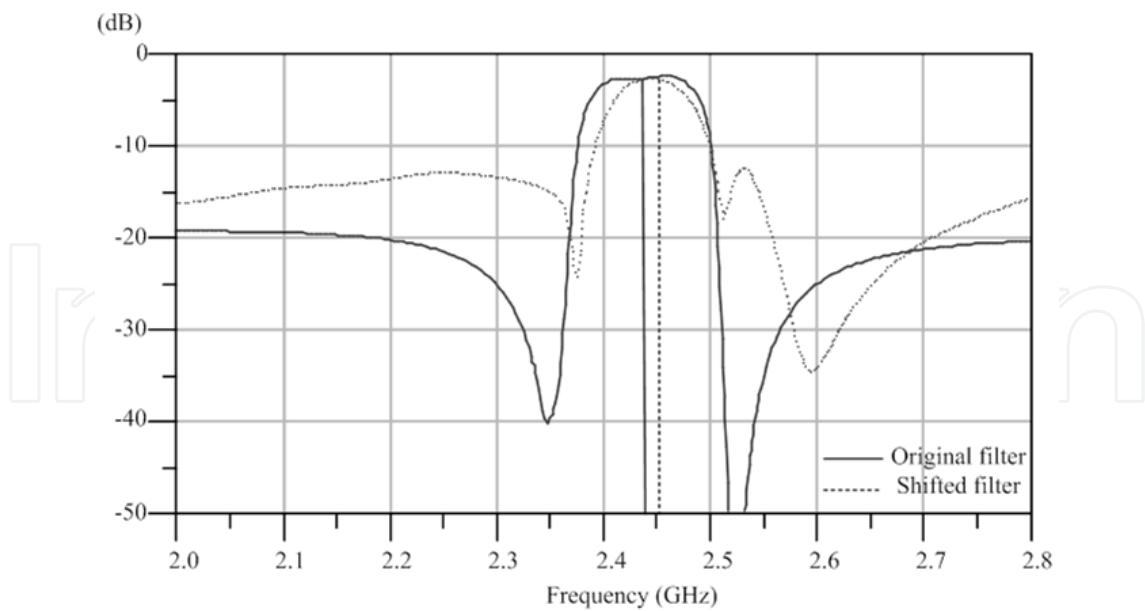

Figure 15. Tunable BAW-SMR filter and passive elements mounted on FR4 PCB.

Fig.16 shows the simulation results of the tunable filter. The insertion loss (IL = -2.4 dB) obtained in the simulation is due to quality factors of resonators (Q = 500). The return loss (RL) is -10 dB, and the out of band rejection is 26 dB at 2.0 GHz. The simulation results shows that a shift of +1% of the initial central frequency (2.44 GHz) is obtained.
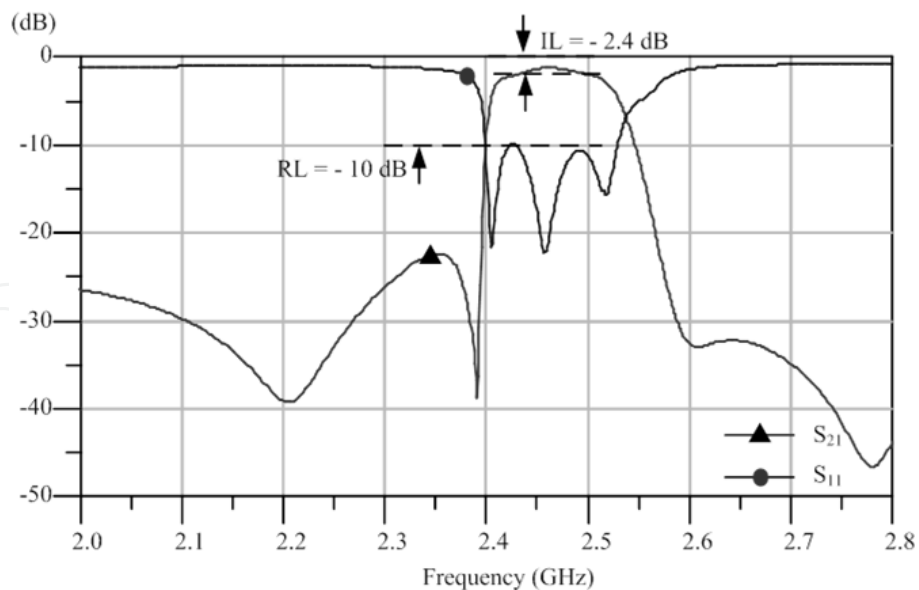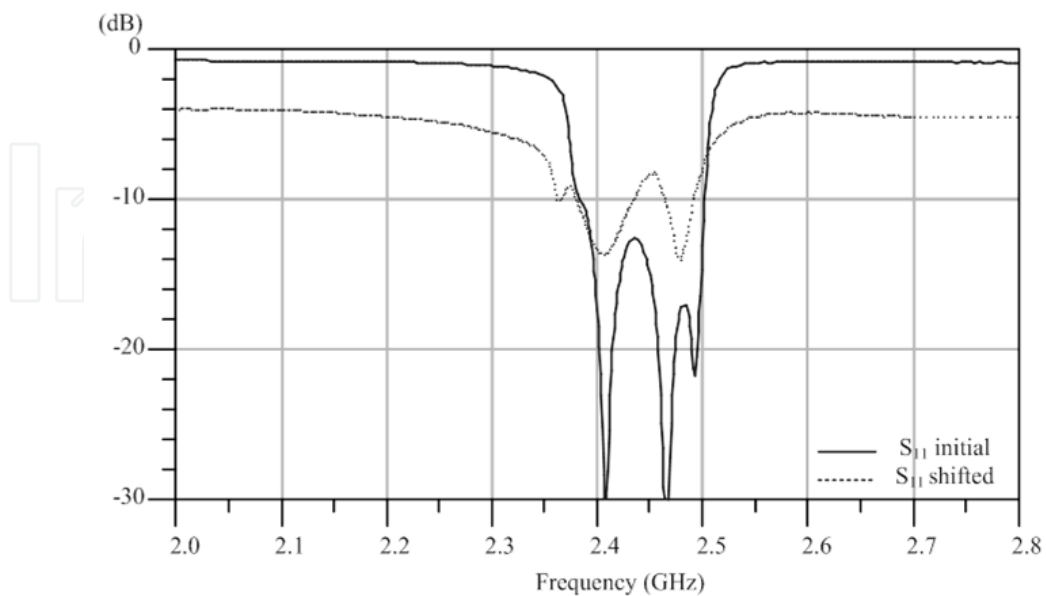

Figure 16. Simulation of tunable BAW filter with inductors added in parallel with the series resonators and capacitors added in series with the shunt resonators.

Comparisons between the measurements of the tunable filter with the original one are shown in Fig.17 and Fig.18.

Figure 17. Shift towards higher frequencies: Comparison of transmission characteristic (S₂₁)between the tunable BAW-SMR filter (passive elements added) and the original one.

Based on the measurements of the tunable filter, we can note -4.5 dB of insertion losses and a shift of +0.6% of the center frequency (2.44 GHz) towards the higher frequencies (Fig.17). As well, a return loss of -7 dB is obtained (Fig.18). The filter high insertion losses are mainly due to the low resonators quality factor obtained in the fabrication (Q = 200) and to the low quality factor of the passive element used. Moreover, the parasitic capacitors generated by the FR4 PCB and the bonding wires used to connect the tunable filter with the passive elements caused a reduction of 15 MHz to the bandwidth of the tunable filter.

Figure 18. Shift towards higher frequencies: Comparison of reflexion characteristic (S₁₁) between the tunable BAW-SMR filter (passive elements added) and the original one.

4.2. Shift towards lower frequencies

This time and in order to shift the center frequency of the filter towards lower frequencies, we have to move all the zeroes towards these frequencies.
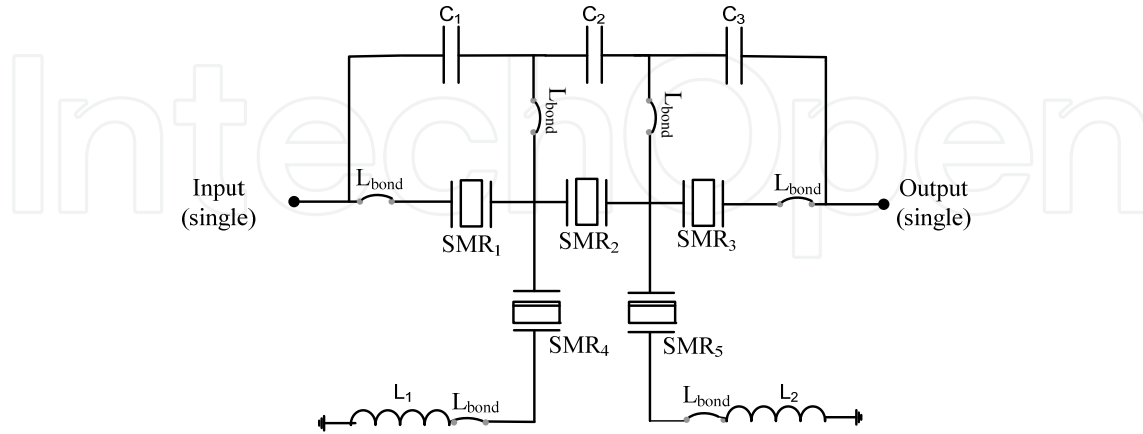
Figure 19. Tunable BAW-SMR filter with capacitors added in parallel with the series resonators and inductors added in series with the shunt resonators.

Thus, we have added capacitors in parallel with the series resonators and inductors in series with the shunt resonators that constitute the ladder BAW-SMR filter (Fig.19). Table 2 presents the values and the quality factor of the external passive elements used.

|	Value	Quality Factor 'Q'
Capacitors	C_1=2.2 pF	140
	C_2=1 pF	200
	C_3=2 pf	150
Inductors	L_1=L_2=2.2 nH	57

Table 2. Values of the passive elements used to shift the center frequency of the tunable BAW-SMR filter towards lower frequencies and their quality factors.

As same as before, the tunable BAW-SMR filter and the passive components are mounted on a FR4 substrate. Fig.20 shows the simulation results of the tunable filter.

The insertion loss (IL = -2.4 dB) obtained by simulation is due to quality factors of resonators (Q = 500). In addition the return loss (RL) is -9.5 dB, and the out of band rejection is 16 dB at 2.0 GHz (Fig.20). The simulation results shows that a shift of -1% of the initial central frequency (2.44 GHz) is obtained. A comparison between the measurements of the tunable filter with the original one is shown in Fig.21.

Based on the measurements of the tunable filter, we can note -4.5 dB of insertion losses and a shift of -1.3% of the center frequency (2.44 GHz) towards the lower frequencies (Fig.21). In addition, the parasitic capacitors generated by the FR4 PCB and the bonding wires used to connect the tunable filter with the passive elements caused a reduction of 13 MHz to the bandwidth of the tunable filter.
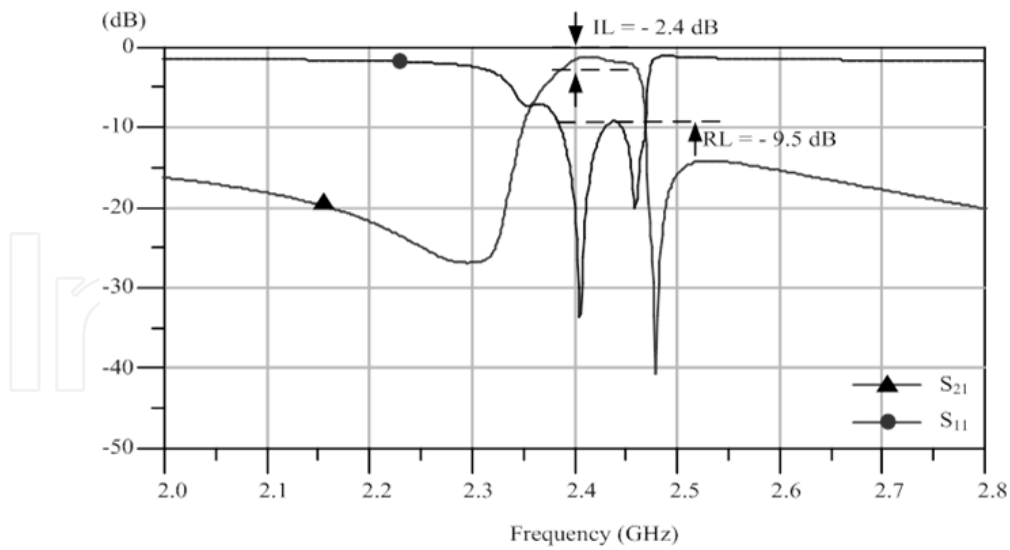
Figure 20. Simulation of tunable BAW filter with capacitors added in parallel with the series resonators and inductors added in series with the shunt resonators.
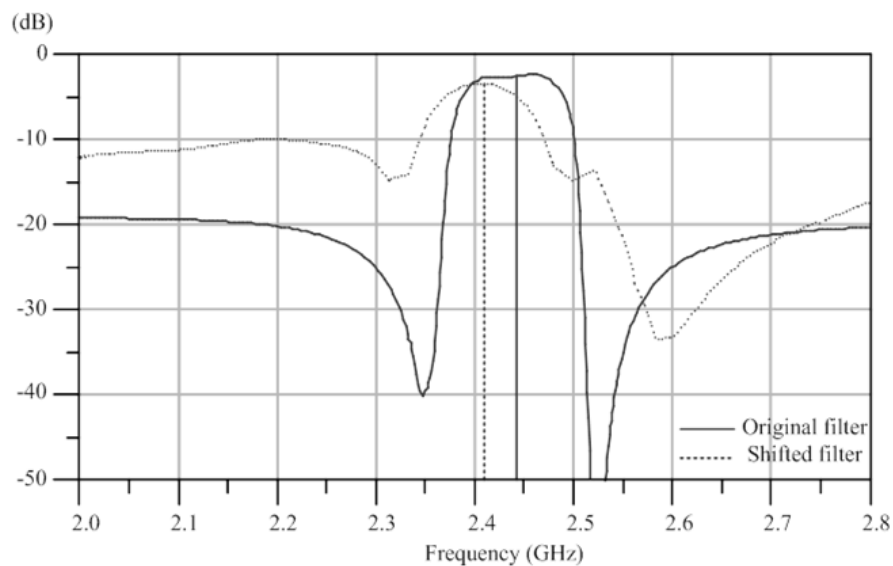

Figure 21. Shift towards lower frequencies: Comparison between the tunable BAW-SMR filter (passive elements added) and the original one.

As a conclusion, one should note that in contrast to [13], where lumped elements (inductors or capacitors) were proposed to be added at a time, in this paper the use of capacitors and inductors together have shown how to shift the center frequencies towards higher or lower frequencies.

5. Digitally tuning BAW filters

To validate the concept of digitally tuning BAW filters using passive elements controlled by CMOS transistors, we present in this part the use of CMOS switches at the terminals of capacitors (Fig.22) [6].

When a transistor is ON, the capacitor is short circuited, and when a transistor is OFF, the capacitor will be considered in series with the shunt resonator. Thus, the bandwidth and the characteristics of the filter will be modified. The circuitry of the filter, capacitors, transistors and the associated "bonding wires" are shown in Fig.22.
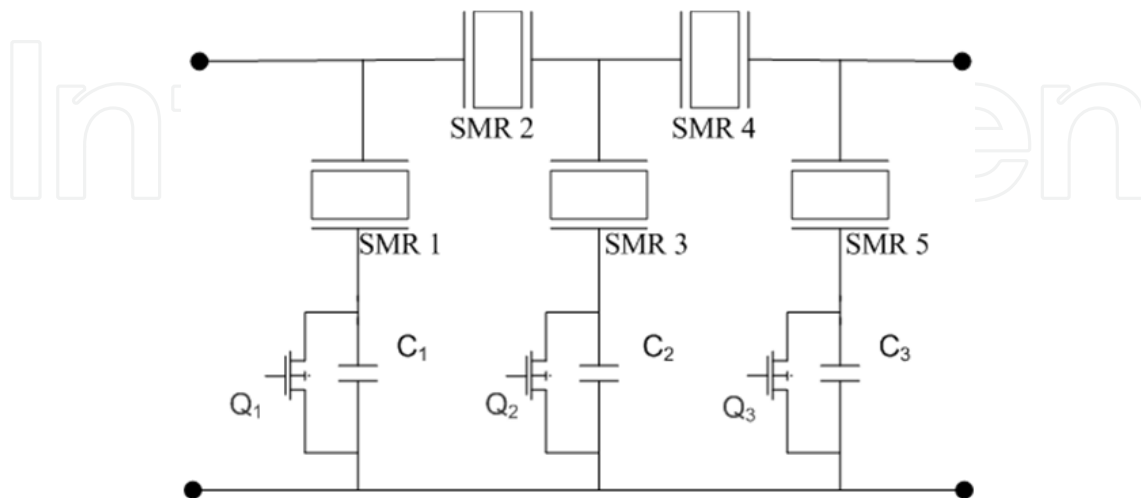
Figure 22. Tunable BAW-SMR using CMOS transistors.

The BAW-SMR filter used in this study is a fifth order filter designed for the W-CDMA standard in the ladder topology. This topology is composed by the resonator in series and parallel, the parallel resonators are loaded and their resonance frequencies are smaller than the series resonators. The die photography of the tunable BAW-SMR filter is shown in Fig.23. The filter has reduced size, and the die area is 1450*985 μm². Moreover, many passive pads connecting the filter with the active chip were taken in consideration.
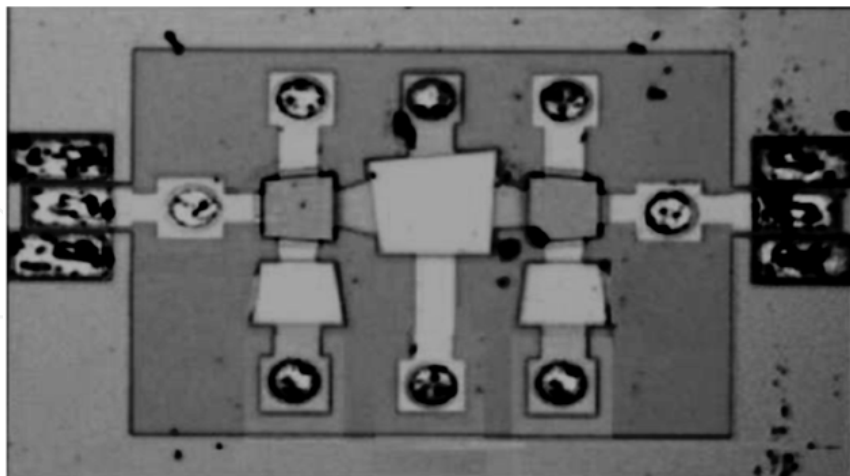
Figure 23. Microphotography of ladder BAW-SMR for the W-CDMA standard.

Fig.24 presents the comparison between the measurement and the simulation of the BAW-SMR filter. Electromagnetic simulation of the overall filter structure has been accomplished by using the ADS-Momentum software, where the acoustical effects have been included using the Mason Model. The filter is designed for implementation in SiP context. As shown

in Fig.24, the measurements are in concordance with the simulations. However, the filter fulfills the requirements for the W-CDMA standard, exhibiting -2.77 dB of insertion loss, -8.75 dB of return loss and selectivity higher than 38 dB at 40MHz offset from the operating frequency.
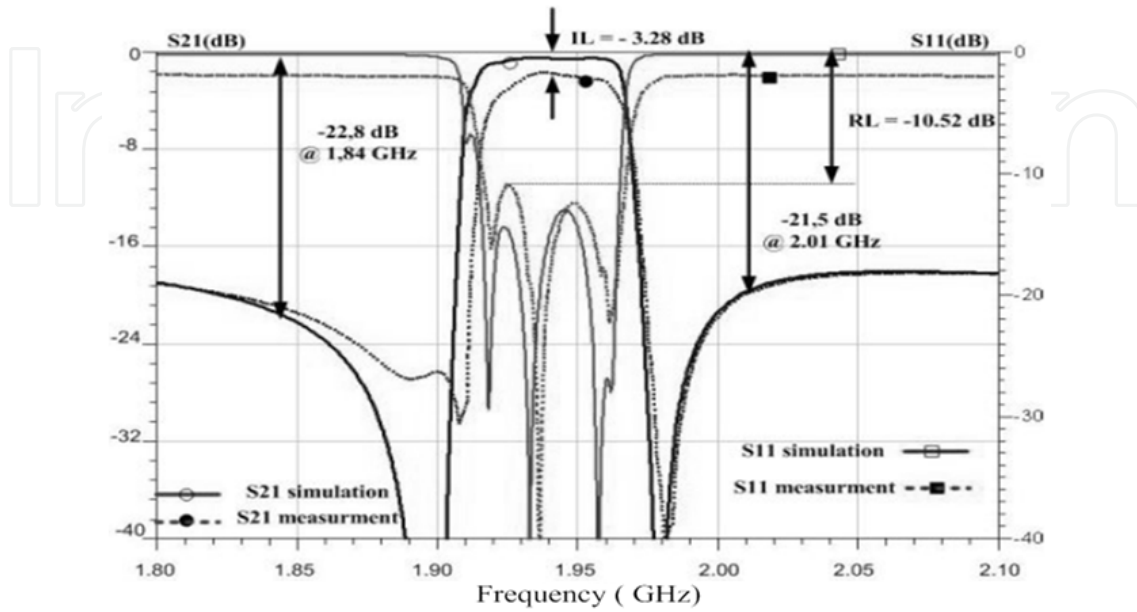

Figure 24. Simulation and measurement results of the W-CDMA ladder BAW-SMR filter.

5.1. Switches design

To adjust the bandwidth of the BAW filter, a chip is realized in 65nm CMOS technology. This chip is composed by the capacitors mounted in series with the MOS transistor, and these transistors are controlled by a 2 to 4 decoder (Fig.25).
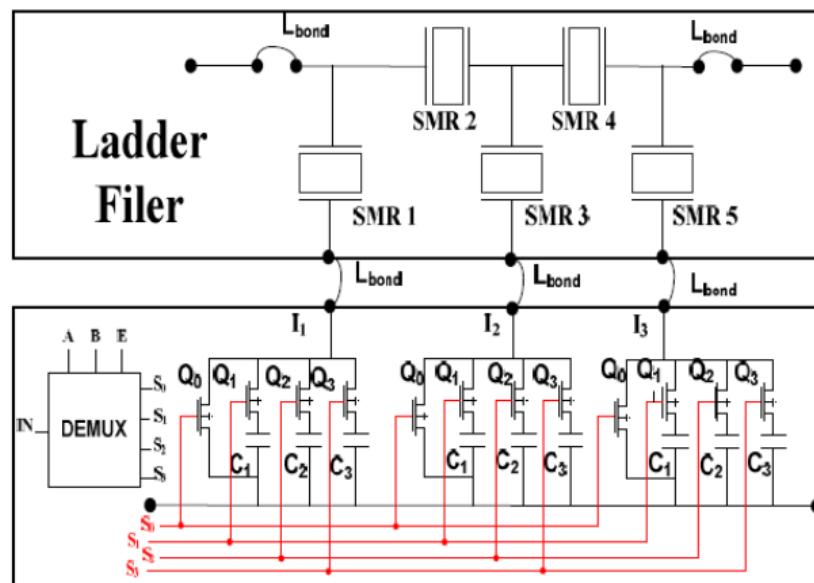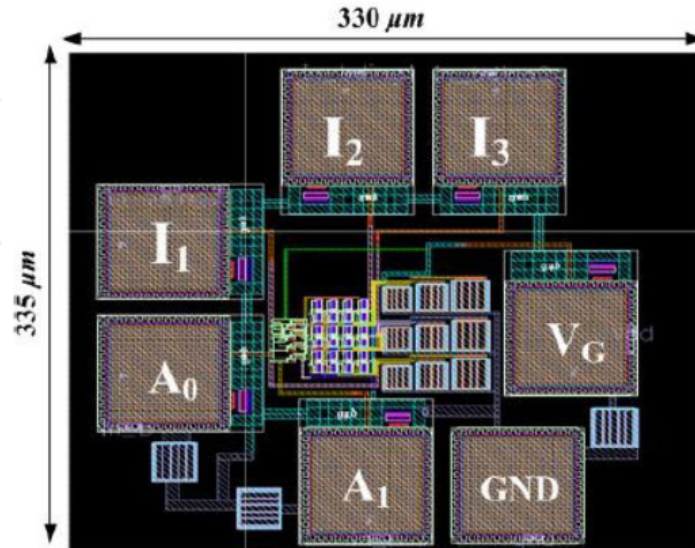

Figure 25. Circuitry of the tuning mechanism.

Fig.26 shows the layout of the tuning circuit. I_n symbolize the pad for connection with ladder filter. V_G, V_{dd1}, V_{dd2} and GND correspond to the gate voltage, the command of decoder and the ground respectively. The size of the Silicon area is 335*330µm².

Figure 26. Layout of the tuning mechanism.

The tuning is attained by controlling the MOS transistors and capacitors in series with shunt resonators. Each transistor is open or short circuited by obtaining different outputs of the 2 to 4 decoder. Table 3 shows the truth table of the realized decoder. A, B, E symbolize the input of a decoder commanded by V_{dd1}, V_{dd2} and V_G respectively, S_n (n = 0, 1, 2 or 3) represent the output of this decoder used to control Q_n. All transistors used in the tuning mechanism are provided by STMicroelectronics (CMOS 65 nm). The width and length of the gate are: W = 50 µm and L = 0.06 µm. The main parasitic elements are taken into account in the simulation (C_{gs}, C_{gd}, C_{ds} and R_{on}). The length of bonding wire is 2 mm. It represents an inductive effect of approximately 2 nH at 2 GHz. R_{on} of the MOS transistor is function of its dimensions and of the gate voltage (V_G). Thus, with an external adjustment of V_G, R_{on} value is regulated.

| A	B	E	S_0	S_1	S_2	S_3
	0	1	0	0	0	1
0	1	1	0	0	1	0
1	0	1	0	1	0	0
1	1	1	1	0	0	0
X	X	0	0	0	0	0

Table 3. Truth table of the 2 to 4 decoder.

5.2. Co-design: BAW filter- 65nm CMOS chip

Fig.27 shows the microphotography of the association of the ladder filter with the active chip. The devices are connected with bonding wires. The capacitors C_1, C_2 and C_3 values are

fixed to achieve 12, 9 and 6 MHz tuning range, respectively. When the output S_0 of the decoder is ON, the transistor Q_0 is ON and all of the capacitors are short circuited. When the output S_n (n = 1, 2 or 3) is ON, the transistor Q_n is ON and the capacitor C_n will be considered in series with the shunt resonators.
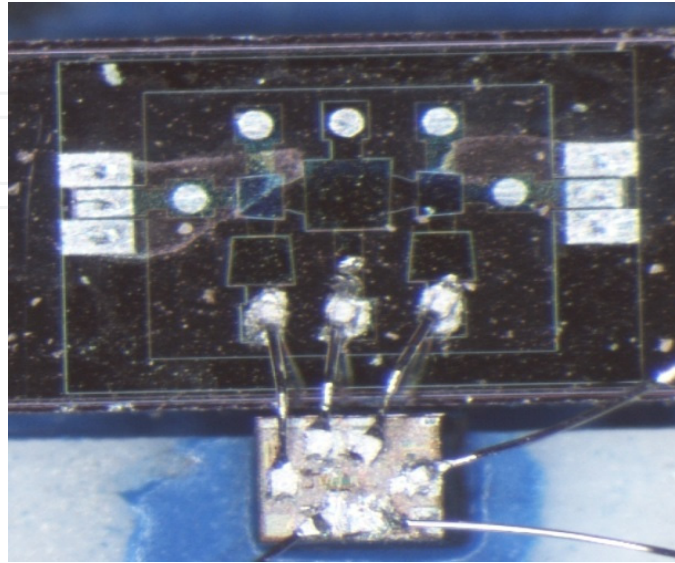
Figure 27. Microphotography of the digitally tunable ladder BAW-SMR for the W-CDMA standard.

The comparison between the simulation and the measurement results is shown in Fig.28. of the tunable BAW-SMR filter combined with the active chip presents a tuning range of 12 MHz, when the output S_3 of the decoder is ON. It show also -1.52 dB of insertion loss and 12 dB of the out-band rejection at 1.85 GHz. This out-band rejection is improved by 3 dB. This degradation is due to the length of bonding wire associating the active chip and PCB [10].
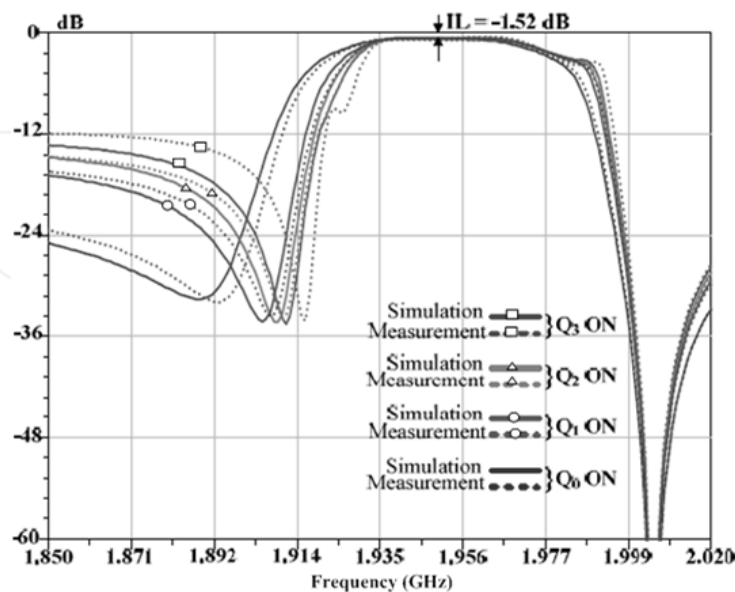
Figure 28. Comparison between the simulation and the measurement of the digitally tunable BAW filter.

6. Conclusion

In this paper, the impedance behavior of the BAW-SMR has been shown. Also, the effects of the addition of passive elements (L, C) to this type of resonators have been illustrated. In addition, a tunable BAW-SMR filter realized in a ladder topology used for the 802.11b/g standard (2.40 - 2.48 GHz) was shown. Mainly, the filter fulfilled the requirements for the WLAN 802.11 b/g standard, presenting a measured -3.3 dB of insertion loss, -12.7 dB of return loss and selectivity higher than 33 dB @ ± 30 MHz of the bandwidth. This tunable BAW-SMR filter has reduced dimensions (1035*1075 µm2). Moreover, the center frequency of this tunable filter was shifted towards higher and lower frequencies by adding passive elements. Measured shifts of -1.3% of the center frequency (2.44 GHz) towards lower frequency and +0.6% of the center frequency towards higher frequencies were obtained. Furthermore, digitally tunable BAW-SMR filter implementation was shown. The tunable filter was designed for the W-CDMA standard. The filter fulfilled the requirements for the WCDMA standard, presenting a measured -2.77 dB of insertion loss, -8.75 dB of return loss and selectivity higher than 38 dB @ ±40 MHz of the bandwidth. Moreover, the center frequency of this tunable filter is digitally shifted towards higher frequencies by adding capacitors in series with transistors that act as switches. These switches are controlled by a 2to4 decoder, and they are added to the shunt resonators.

Author details

M. El Hassan
University of Balamand –Al Kura, Lebanon

E. Kerherve, Y. Deval and K. Baraka
IMS Laboratory – UMR 5218 CNRS – University of Bordeaux, France

J.B. David
CEA-Leti – Minatec – Grenoble, France

D. Belot
ST Microectronics – Crolles, France

Acknowledgement

7. References

[1] Bradley, P. et al. "A Film acoustic bulk resonator (SMR) duplexer for USPCS Handset Applications", *IEEE MTT-S*, pp.367–370, 2001.

[2] Carpentier, J. F. et al. "A SiGe:C BICMOS WCDMA zero-IF RF front-end using an above-IC BAW filter", *IEEE ISSCC,* 2005, pp. 394-395.

[3] Shirakawa, A. A. Jarry, P. Pham, J-M. Kerherve, E. Dumont, F. David, J-B. Cathelin, A. "Ladder-Lattice Bulk Acoustic Wave Filters: Concepts, Design and Implementation", *RF and Microwave Computer Aided Engineering*, 2007.Newell, "Face-mounted piezoelectric resonators", Proc. IEEE, Vol 53, June 1965, pp.575-581.

[4] Newell, "Face-mounted piezoelectric resonators", Proc. IEEE, Vol 53, June 1965, pp.575-581.

[5] Lakin, K.M. Kline, G. McCarron, K.T. "High-Q microwave acoustic resonators and filter", *IEEE Trans. On Microwave Theory and Techniques*, vol. 41, pp. 2139-2146, Dec. 1993.

[6] Lakin, K.M. Belsick, J. McDonald, J.F. McCarron, K.T. "Improved bulk wave resonator coupling coefficient for wide bandwidth filters", *IEEE Ultrasonics Symposium*, Atlanta, GA, USA, pp.827-831, October 9, 2001.

[7] Fattinger G. G. et al. "Thin Film Bulk Wave Devices for Applications at 5.2 GHz", *IEEE UFFC Symposium*, Honolulu, Hawaii, pp. 174-177, 2003.

[8] Ancey, P. "Above IC RF MEMS and BAW filters: fact or fiction", *IEEE BCTM Proceedings*, Maastricht, Netherlands, pp. 186-190, 2006.

[9] Shirakawa, A. A. Pham, J-M. Jarry, P. Kerherve, E. Dumont, F. David, J-B. Cathelin, A."A High Isolation and High Selectivity Ladder-Lattice BAW-SMR Filter", *36th European Microwave Conference,* 2006, Manchester, UK, pp. 905 – 908, 10-15 September.

[10] Tsutsumi, J. Iwaki, M. Iwamoto, Y. Yokoyama, T. Sakashita, T. Nishihara, T. Ueda, M. Satoh, Y. "A Miniaturized FBAR Duplexer with Reduced Acoustic Loss for the W-CDMA Application", *IEEE Ultrasonics Symposium Proceedings,* Rotterdam, Netherlands, pp. 93-96, 2005.

[11] Lakin, K. M. Lakin, K. G. "Numerical Analysis of Thin Film BAW Resonators", *Proceedings of Ultrasonics Symposium*, Honolulu, Hawaii, Vol. 1, pp. 74-79, 2003.

[12] Mason, W. P. "Electromechanical Transducers and Wave Filters", Princeton, New Jersey, Van Nostrand, 1948.

[13] El Hassan, M. Kerherve, E. Deval, Y. David, J.B. Belot, D. "Reconfiguration of Bulk Acoustic Wave Filters Using CMOS Transistors: Concept, Design and Implementation", 2010 IEEE RFIC Symposium, Anaheim, CA, USA, 23 - 25 May, 2010. pp. 241 – 244.